Hindawi
Complexity
Volume 2022, Article ID 2417748, 14 pages
https://doi.org/10.1155/2022/2417748

Research Article

Vibration Suppression of a Coupled Aircraft Wing with Finite-Time Convergence

Yiming Liu, Zhifeng Tan, Xiaofen Yang, and Xiaowei Wang

School of Mechanical and Electric Engineering, Guangzhou University, Guangzhou 510006, China

Correspondence should be addressed to Xiaowei Wang; meewxw_ee@gzhu.edu.cn

Received 6 August 2021; Accepted 9 September 2021; Published 16 February 2022

Academic Editor: Zhenyu Lu

A nonlinear coupled wing model subject to unknown external disturbances is proposed in this paper. Since the model is modeled by partial differential equations, the traditional control design scheme based on the ordinary differential equation model is not applicable, and the control law design becomes very complex. In this paper, a new antidisturbance boundary control scheme based on a finite time convergent disturbance observer is proposed. The control laws are designed based on the new disturbance observers to make the external disturbance errors converge to zero in a finite time and ensure the uniformly bounded stability of the controlled system. Finally, the effectiveness of the controllers and the finite-time convergence of disturbance errors are verified by the simulation and comparison.

1. Introduction

Due to the characteristics of maneuverability, flexibility, and wide vision, aircrafts are widely used in various fields. Aircrafts include the fixed-wing, rotary-wing, and flapping-wing aircraft. Among them, the flapping-wing aircraft has unique advantages, including higher flight maneuverability and low flight costs. In addition, although the size is small and the flight resistance is large, the flight efficiency of the flapping-wing aircraft will not be reduced [1]. Therefore, more and more researchers are engaged in the research of flapping-wing aircraft [2–6]. Researchers combined the structural design with bionics to develop and research the flapping-wing aircraft. Some researchers used rigid materials to make the wings, which ignored the influence of fluid dynamic changes caused by the deformation of insect wings so that the fuselage may not be flexible enough and prone to failure during execution [7]. Because flexible materials have the advantages of improving the running speed of the mechanical system and further reducing the weight of the structure, they are widely used in the mechanical structure manufacturing in recent years [8, 9]. Therefore, we can use flexible materials to make flapping-wing aircraft wings [10]. Although the flexible wing can improve the flexibility of flapping-wing aircraft, the vibration and deformation of wings will affect the control effect and flight performance. Consequently, the problem of wing vibration needs to be solved urgently, which inspired our research. In this paper, we regard a single wing as a coupled distributed parameter system and use the combination of partial differential equation and ordinary differential equation (PDE-ODE) to describe the wing dynamic model. Due to the complexity of distributed parameter system control design, more and more attention has been paid in recent years [11–21].

For the problem of vibration suppression of distributed parameter systems, several researchers have proposed various control methods including the modal reduction method [22] and boundary control [23–29]. The modal reduction method can effectively reduce the order of the infinite-dimensional system and treat the system as a finite dimension, but this method can easily cause spillover effects. The boundary control strategy can effectively solve this problem and improve the robustness of the system. In recent years, the research on vibration suppression of flexible structural systems based on the boundary control has made great progress. For example, in [30], with the method of barrier Lyapunov function, the controller could suppress the vibration of the system and cope with the input and output

constraints at the same time. In [31], a boundary controller was constructed to suppress the vibration excursion of the hose using the backstepping control method, and a smooth hyperbolic tangent function was introduced to cope with the input amplitude and rate constraints. In [32], a boundary control was designed for the flexible string system with vibration and input backlash. In [33], with the help of a new disturbance observer, the external disturbance was effectively suppressed, and the purpose of vibration reduction was achieved. A robust adaptive controller was proposed to deal with parameter uncertainties and stabilize the system in [34]. In [35], the authors put forward an adaptive NN control strategy for flexible string systems with input constraints and actuator failures. Two iterative learning boundary control schemes were designed for a flexible microair vehicle under spatiotemporal variation disturbances to suppress structural vibration and make it track the target trajectory in [36]. As for the boundary control of the flexible aircraft wing system, many scholars have researched in recent years [37–39]. However, these studies did not consider that the system was affected by both distributed disturbances and boundary disturbances, and their existence may bring great side effects to the system. Therefore, disturbance suppression has become a key problem in the wing control design.

In the past few years, one of the most commonly used antidisturbance methods is the disturbance observer technique. This method can be used for nonlinear systems with uncertainties and efficiently improve the robustness of the system [40–42]. The boundary disturbance observer-based control problem of a vibrating single-link flexible manipulator system with external disturbances was studied in [43]. In [44], considering the influence of extraneous disturbance acting on the wing, a new observer was proposed for controller design. A new disturbance observer was proposed to deal with the distributed disturbance and boundary disturbance of a flexible-link manipulator in [45]. However, it is noted that although the disturbance observer proposed in the above research could effectively track the change of unknown disturbance, it must be assumed that the disturbance changes slowly, and it could not ensure that the disturbance error converged in a finite time. For systems affected by the external disturbance with unknown varying frequency, it is very important to ensure that the disturbance error converges in a finite time [46]. So far, there has been no research on the finite-time convergence control of the coupled aircraft wing system, which motivates this research.

In this article, the stability of nonlinear flexible coupled wing systems under external disturbances is studied. We briefly describe the contributions of this work: (i) Considering the unknown boundary disturbances of the flexible wing, the model is updated on this basis. (ii) The proposed observer can guarantee that the disturbance errors can converge to zero in a finite time. (iii) The vibration problem of the wing structure is well solved, and there is no spillover effect in the system control.

The rest of this paper is organized as follows: the dynamics of the coupled aircraft wing system are presented in Section 2. Section 3 presents the new finite-time control scheme and a detailed analysis of the stability of the closed-loop system. Simulation and analysis are carried out in Section 4. Finally, the conclusion is given in Section 5.

2. Problem Statement

2.1. System Model. A vibrating flexible flapping-wing aircraft subject to unknown disturbances is depicted in Figure 1. In this paper, $\mathscr{R}$ represents a collection of real numbers, $x_e c$ is the length between the shear center and the mass center of the wing cross section, and $x_a c$ is the distance from the aerodynamic center to the shear center of the wing. ρ is the mass per unit of the wing, I_p describes the polar moment of inertia, EI_b denotes the bending rigidity, GJ represents torsion rigidity, $g_h(z,t)$ denotes the distributed disturbance, ξ represents the Kelvin–Voigt damping coefficient, and $\tau_1(t)$ and $\tau_2(t)$ represent the control inputs. Besides, $g_1(t)$ and $g_2(t)$ are the unknown disturbances at the wing tip $z = s$. For simplicity, some symbols are replaced with $\dot{(\cdot)} = \partial(\cdot)/\partial t$, $(\cdot)' = \partial(\cdot)/\partial z$, $\dot{(\cdot)}' = \partial^2(\cdot)/\partial z\,\partial t$, $(\cdot)'' = \partial^2(\cdot)/\partial z^2$, and $\ddot{(\cdot)} = \partial^2(\cdot)/\partial t^2$.

The kinetic energy $E_k(t)$ of the flexible wing in this study is given directly as follows:

$$E_k(t) = \frac{1}{2}\rho \int_0^s [\dot{q}(z,t)]^2 \mathrm{d}z + \frac{1}{2} I_p \int_0^s [\dot{\theta}(z,t)]^2 \mathrm{d}z. \tag{1}$$

$E_p(t)$ denotes the potential energy of the flexible wing:

$$E_p(t) = \frac{1}{2} EI_b \int_0^s [q''(z,t)]^2 \mathrm{d}z + \frac{1}{2} GJ \int_0^s [\theta'(z,t)]^2 \mathrm{d}z. \tag{2}$$

The virtual work of damping on the wing is expressed by

$$\begin{aligned} \delta H_d(t) = &-\xi EI_b \int_0^s \dot{q}''(z,t)\delta q''(z,t)\mathrm{d}z \\ &- \xi GJ \int_0^s \cdot \theta'(z,t)\delta\theta'(z,t)\mathrm{d}z. \end{aligned} \tag{3}$$

The virtual work of the coupling of bending and torsion stiffness is presented as follows:

$$\begin{aligned} \delta H_c(t) = &\rho x_e c \int_0^s \ddot{q}(z,t)\delta\theta(z,t)\mathrm{d}z \\ &+ \rho x_e c \int_0^s \ddot{\theta}(z,t)\delta q(z,t)\mathrm{d}z. \end{aligned} \tag{4}$$

The virtual work of unknown disturbance is given as

$$\begin{aligned} \delta H_f(t) = &\int_0^s \left[g_h(z,t)\delta q(z,t) - x_a c g_h(z,t)\delta\theta(z,t)\right]\mathrm{d}z \\ &+ g_1(t)\delta q(s,t) + g_2(t)\delta\theta(s,t). \end{aligned} \tag{5}$$

The virtual work $\delta H_\tau(t)$ performed by the control inputs can be obtained as follows:

$$\delta H_\tau(t) = \tau_1(t)\delta q(s,t) + \tau_2(t)\delta\theta(s,t). \tag{6}$$

Then, we add all the virtual works of the system:

$$\delta H(t) = \delta\left[H_c(t) + H_d(t) + H_f(t) + H_\tau(t)\right]. \tag{7}$$

Hamilton's principle is formulated as follows [47, 48]:

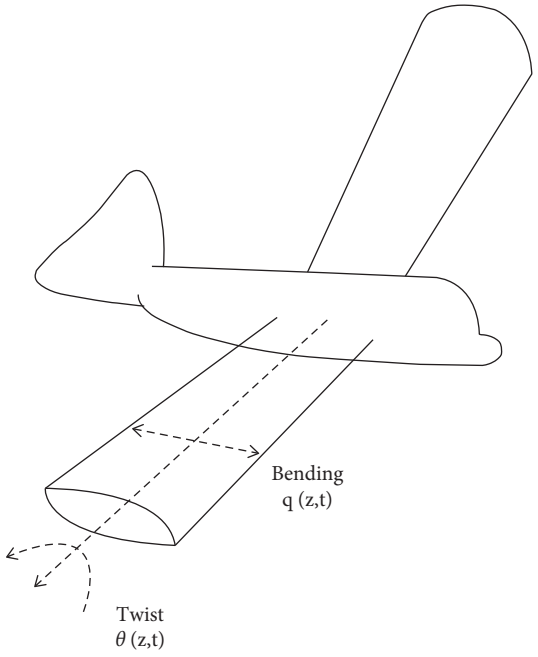

Figure 1: Flapping-wing robotic aircraft.

$$\int_{t_1}^{t_2} \delta\left[E_k(t) - E_p(t) + H(t)\right]\mathrm{d}t = 0. \tag{8}$$

According to (8), we can obtain the flexible wing dynamics as follows:

$$\begin{aligned} &I_p\ddot{\theta}(z,t) - GJ\theta''(z,t) - \rho x_e c\ddot{q}(z,t) \\ &\quad - \xi GJ\dot{\theta}''(z,t) = -x_a c g_h(z,t), \\ &\rho\ddot{q}(z,t) + EI_b q'''' \\ &\quad - \rho x_e c\ddot{\theta}(z,t) + \xi EI_b\dot{q}''''(z,t) = g_h(z,t). \end{aligned} \tag{9}$$

Moreover, we can get the boundary conditions of the system:

$$\begin{aligned} &q(0,t) = q'(0,t) = q''(s,t) = \theta(0,t) = 0, \\ &EI_b q'''(s,t) + \xi EI_b\dot{q}'''(s,t) = -\tau_1(t) - g_1(t), \\ &GJ\theta'(s,t) + \xi GJ\dot{\theta}'(s,t) = \tau_2(t) + g_2(t). \end{aligned} \tag{10}$$

2.2. Preliminaries. The lemmas and assumption are proposed here to facilitate the later controller design and stability analysis.

Assumption 1. For $g_1(t)$, $g_2(t)$, and $g_h(z,t)$, we suppose that there exist $\zeta_1 > 0$, $\zeta_2 > 0$, and $g_{h\max} > 0$ such that $|g_1(t)| \le \zeta_1$, $|g_2(t)| \le \zeta_2$, and $|g_h(z,t)| \le g_{h\max}$, $(z,t) \in t[0,s]n \times q[0,+\infty)$. This assumption is reasonable because the energy of external disturbances is limited.

Lemma 1 (see [49]). *If there exist $\varpi_1(s,t), \varpi_2(s,t) \in \mathscr{R}$, $p > 0$ with $(s,t) \in t[0,f]n \times q[0,+\infty)$, we can obtain*

$$\varpi_1\varpi_2 \le \frac{1}{p}\varpi_1^2 + p\varpi_2^2. \tag{11}$$

Lemma 2 (see [49]). *If $\varpi(s,t) \in \mathscr{R}$ satisfies the condition $\varpi(0,t) = 0$, then*

$$\varpi^2 \le f\int_0^f \varpi'^2\mathrm{d}s, \tag{12}$$

where $(s,t) \in t[0,f]n \times q[0,+\infty)$.

Lemma 3. *The following inequality for the positive definite function $Q(t)$ is used to derive our main results as follows:*

$$\dot{Q}(t) \le -\phi_1 Q(t) - \phi_2 Q^{\phi_3}(t). \tag{13}$$

Then, the function $Q(t)$ will have an equilibrium point. It can converge to the point in a finite time as follows:

$$t_f \le \frac{1}{\phi_1(1-\phi_3)}\ln\frac{\phi_1 Q^{1-\phi_3}(0) + \phi_2}{\phi_2}, \tag{14}$$

with $\phi_1 > 0$, $\phi_2 > 0$, and $0 < \phi_3 < 1$ being undetermined constants.

3. Control Design

The emphasis of the research is how to construct boundary controllers to suppress the vibration of a coupled wing system. For the sake of the control goal, a new control scheme based on finite-time disturbance observer is adopted, which can ensure the stability of the closed-loop system. The control block diagram of the system is shown in Figure 2.

First, the boundary control laws are proposed as follows:

$$\begin{aligned} \tau_1(t) &= -k_1[aq(s,t) + b\dot{q}(s,t)] - \widehat{g}_1(t), \\ \tau_2(t) &= -k_2[a\theta(s,t) + b\dot{\theta}(s,t)] - \widehat{g}_2(t), \end{aligned} \tag{15}$$

where $k_1, k_2 > 0$.

Step 1. The auxiliary functions are defined as follows:

$$\sigma_1(t) = -\xi EIq'''(s,t) - \nu_1(t), \tag{16}$$

$$\begin{aligned} \dot{\nu}_1(t) = {} & \kappa_1\sigma_1(t) + \kappa_2\mathrm{sign}\left(\sigma_1(t)\right) + \kappa_3\sigma_1^{2a_1 - a_2/a_2}(t) \\ & + \tau_1(t) + EI_b q'''(s,t), \end{aligned} \tag{17}$$

$$\sigma_2(t) = \xi GJ\theta'(s,t) - \nu_2(t), \tag{18}$$

$$\begin{aligned} \dot{\nu}_2(t) = {} & \kappa_4\sigma_2(t) + \kappa_5\mathrm{sign}\left(\sigma_2(t)\right) + \kappa_6\sigma_2^{2b_1 - b_2/b_2}(t) \\ & + \tau_2(t) - GJ\theta'(s,t). \end{aligned} \tag{19}$$

To arrive at the control objectives that deal with the unknown disturbances $g_1(t)$ and $g_2(t)$, we define the estimation form of disturbance terms as follows:

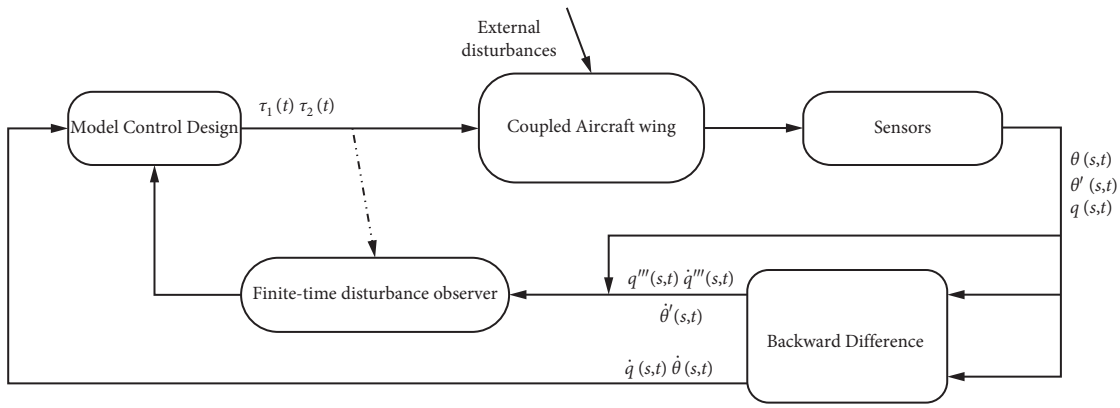

Figure 2: Finite-time control for the coupled aircraft wing.

$$\widehat{g}_1(t) = \kappa_1\sigma_1(t) + \kappa_2\text{sign}\left(\sigma_1(t)\right) + \kappa_3\sigma_1^{2a_1-a_2/a_2}(t), \tag{20}$$

$$\widehat{g}_2(t) = \kappa_4\sigma_2(t) + \kappa_5\text{sign}\left(\sigma_2(t)\right) + \kappa_6\sigma_2^{2b_1-b_2/b_2}(t), \tag{21}$$

where $\kappa_1, \kappa_2, \kappa_3, \kappa_4, \kappa_5$, and κ_6 are all positive numbers. Moreover, a_1, a_2, b_1, and b_2 are all odd numbers that satisfied $a_1 < a_2 < 2a_1$ and $b_1 < b_2 < 2b_1$.

Step 2. We choose Lyapunov candidate function as

$$W(t) = W_a(t) + W_o(t), \tag{22}$$

where

$$\begin{aligned} W_a(t) &= \frac{b}{2}\rho\int_0^s [\dot{q}(z,t)]^2\mathrm{d}z + \frac{b}{2}EI_b\int_0^s [q''(z,t)]^2\mathrm{d}z + \frac{b}{2}I_p\int_0^s [\dot{\theta}(z,t)]^2\mathrm{d}z + \frac{b}{2}GJ\int_0^s [\theta'(z,t)]^2\mathrm{d}z, \\ W_o(t) &= a\rho\int_0^s \dot{q}(z,t)q(z,t)\mathrm{d}z + aI_p\int_0^s \dot{\theta}(z,t)\theta(z,t)\mathrm{d}z \\ &\quad - a\rho x_e c\int_0^s [\dot{q}(z,t)\theta(z,t) + q(z,t)\dot{\theta}(z,t)\mathrm{d}z - bx_e c\int_0^s \dot{q}(z,t)\dot{\theta}(z,t)\mathrm{d}z, \end{aligned} \tag{23}$$

where $a > 0$ and $b > 0$.

Remark 1. In this paper, we use the Lyapunov direct method to design the controller given in the specific form of Lyapunov function, where $W_a(t)$ is derived from the system kinetic energy $E_k(t)$ and potential energy $E_p(t)$, which is called the energy term. $W_o(t)$ is derived from the coupling of various state quantities of the system and becomes a crossing term. $Q_1(t)$ and $Q_2(t)$ will be given later in this article, which represent the auxiliary items of the system to deal with disturbance errors. By adjusting the control laws (15)–(21) and Lyapunov candidate function, we ensure that the derivative of Lyapunov function $W(t)$ has an upper bound and let $Q_1(t)$ *and* $Q_2(t)$ satisfy Lemma 3 so as to prove the uniform boundedness of state variables and the finite-time convergence of disturbance errors.

Remark 2. The control signals $q(s,t), \dot{q}(s,t), \theta(s,t), \dot{\theta}(s,t), q'''(s,t), \theta'(s,t), \dot{q}'''(s,t)$, and $\dot{\theta}'(s,t)$ in the control equations (15)–(21) can be obtained during execution, where $q(s,t)$ and $\theta(s,t)$ are obtained by the laser displacement sensors, and $\theta'(s,t)$ is obtained by the inclinometer. The remaining variables $\dot{q}(s,t), \dot{\theta}(s,t), q'''(s,t), \dot{q}'''(s,t)$, and $\dot{\theta}'(s,t)$ are further obtained by the backward difference algorithms.

Theorem 1. *The Lyapunov function (22) has upper and lower bounds:*

$$0 \le \lambda_2\kappa(t) \le W(t) \le \lambda_1\kappa(t), \tag{24}$$

where λ_1 *and* λ_2 *are positive numbers.*

Proof. A new function is defined as follows:

$$\kappa(t) = \int_0^s \left\{ [\dot{q}(z,t)]^2 + [q''(z,t)]^2 + [\dot{\theta}(z,t)]^2 + [\theta'(z,t)]^2 \right\}\mathrm{d}z. \tag{25}$$

Hence, we obtain

$$y_2\kappa(t) \le W_a(t) \le y_1\kappa(t), \tag{26}$$

where y_1 and y_2 are two positive numbers, $y_1 = (b/2)\max\{EI_b, I_p, GJ, \rho\}$, and $y_2 = (b/2)\min\{\rho, EI_b, I_p, GJ\}$. For $W_o(t)$, we can obtain

$$\begin{aligned}|W_o(t)| \le\ & a\rho\left\{\int_0^s [\dot{q}(z,t)]^2 \mathrm{d}z + s^4 \int_0^s [q''(z,t)]^2 \mathrm{d}z\right\} + aI_p\left\{\int_0^s [\dot{\theta}(z,t)]^2 \mathrm{d}z + s^2 \int_0^s [\theta'(z,t)]^2 \mathrm{d}z\right\} \\ & + a\rho x_e c\left\{\int_0^s [\dot{q}(z,t)]^2 \mathrm{d}z + \int_0^s [\dot{\theta}(z,t)]^2 \mathrm{d}z\right\} + a\rho x_e c\left\{s^4 \int_0^s [q''(z,t)]^2 \mathrm{d}z + s^2 \int_0^s [\theta'(z,t)]^2 \mathrm{d}z\right\} \\ & + b\rho x_e c\left\{\int_0^s [\dot{q}(z,t)]^2 \mathrm{d}z + \int_0^s [\dot{\theta}(z,t)]^2 \mathrm{d}z\right\} + \left(aI_p + a\rho x_e c + b\rho x_e c\right) \int_0^s [\dot{\theta}(z,t)]^2 \mathrm{d}z + \left(aI_p + a\rho x_e c\right)s^2 \\ & \cdot \int_0^s [\theta'(z,t)]^2 \mathrm{d}z \le y_3 \kappa(t),\end{aligned} \tag{27}$$

where $y_3 = \max\{a\rho + a\rho x_e c + b\rho x_e c,\ (a\rho + a\rho x_e c)s^4, aI_p + a\rho x_e c + b\rho x_e c, (aI_p + a\rho x_e c)s^2\}$ and b satisfies $b > 2y_3/\min\{\rho, I_p, EI_b, GJ\}$.

Now, we can prove equation (24) as follows:

$$O \le \lambda_2 \kappa(t) \le W(t) \le \lambda_1 \kappa(t), \tag{28}$$

where $\lambda_2 = y_2 - y_3$ and $\lambda_1 = y_1 + y_3$. □

Step 3. The derivative of $W_a(t)$ gives

$$\begin{aligned}\dot{W}_a(t) \le\ & -b\dot{q}(s,t)\left[EI_b q'''(s,t) + \xi EI_b \dot{q}'''(s,t)\right] + b\dot{\theta}(s,t)\left[GJ\theta'(s,t) + \xi GJ\dot{\theta}'(s,t)\right] \\ & + b\rho x_e c \int_0^s [\dot{q}(z,t)\ddot{\theta}(z,t) + \ddot{q}(z,t)\dot{\theta}(z,t)]\mathrm{d}z - \left(\frac{b\xi GJ}{2s^2} - \eta_2 b x_a c\right)\int_0^s [\dot{\theta}(z,t)]^2 \mathrm{d}z - \left(\frac{b\xi EI_b}{2s^4} - \eta_1 b\right)\int_0^s [\dot{q}(z,t)]^2 \mathrm{d}z \\ & + \left(\frac{b}{\eta_1} + \frac{bx_a c}{\eta_2}\right) s g_{h\max}^2 - \frac{b\xi EI_b}{2}\int_0^s [\dot{q}''(z,t)]^2 \mathrm{d}z - \frac{b\xi GJ}{2}\int_0^s \left[\dot{\theta}''(z,t)\right]^2 \mathrm{d}z.\end{aligned} \tag{29}$$

Similarly, differentiating $W_o(t)$ leads to

$$\begin{aligned}\dot{W}_o(t) =\ & a\rho \int_0^s \ddot{q}(z,t)q(z,t)\mathrm{d}z \\ & + aI_p \int_0^s \ddot{\theta}(z,t)\theta(z,t)\mathrm{d}z \\ & - a\rho x_e c \int_0^s \ddot{q}(z,t)\theta(z,t)\mathrm{d}z \\ & - a\rho x_e c \int_0^s q(z,t)\ddot{\theta}(z,t)\mathrm{d}z \\ & + a\rho \int_0^s [\dot{q}(z,t)]^2 \mathrm{d}z + aI_p \int_0^s [\dot{\theta}(z,t)]^2 \mathrm{d}z \\ & - b\rho x_e c \int_0^s \ddot{q}(z,t)\dot{\theta}(z,t)\mathrm{d}z \\ & - b\rho x_e c \int_0^s \dot{q}(z,t)\ddot{\theta}(z,t)\mathrm{d}z \\ & - 2a\rho x_e c \int_0^s [\dot{q}(z,t)\dot{\theta}(z,t)]\mathrm{d}z.\end{aligned} \tag{30}$$

Considering (10) and controllers (15)–(21), we obtain

$$\begin{aligned}\dot{W}(t) \le\ & -\left(k_2 - \frac{1}{\eta_9}\right)[a\theta(s,t) + b\dot{\theta}(s,t)]^2 + \tilde{g}_2^2(t)\eta_9 \\ & -\left(k_1 - \frac{1}{\eta_8}\right)[aq(s,t) + b\dot{q}(s,t)]^2 + \tilde{g}_1^2(t)\eta_8 \\ & -\left(aEI_b - \frac{a\xi EI_b}{\eta_3} - \eta_6 a s^4\right)\int_0^s [q'''(z,t)]\mathrm{d}z \\ & -\left(aGJ - \frac{a\xi GJ}{\eta_4} - \eta_7 s^2 x_a c\right)\int_0^s [\theta'(z,t)]^2 \mathrm{d}z \\ & -\left(\frac{b\xi EI_b}{2s^4} - \eta_1 b - a\rho - 2a\rho x_e c\eta_5\right)\int_0^s [\dot{q}(z,t)]^2 \mathrm{d}z \\ & -\left(\frac{b\xi GJ}{2s^2} - \eta_2 b x_a c - aI_p - \frac{2a\rho x_e c}{\eta_5}\right)\int_0^s [\dot{\theta}(z,t)]^2 \mathrm{d}z \\ & -\left(\frac{b\xi EI_b}{2} - a\xi EI_b\eta_3\right)\int_0^s [\dot{q}''(z,t)]^2 \mathrm{d}z \\ & -\left(\frac{b\xi GJ}{2} - a\xi GJ\eta_4\right)\int_0^s \left[\dot{\theta}'(z,t)\right]^2 \mathrm{d}z \\ & +\left(\frac{b}{\eta_1} + \frac{bx_a c}{\eta_2} + \frac{a}{\eta_6} + \frac{ax_a c}{\eta_7}\right) s g_{h\max}^2 \\ \le\ & -\lambda_3 \kappa(t) + \varepsilon,\end{aligned} \tag{31}$$

where $\eta_i > 0, i = 1 \ldots 9$. In addition, because $\widehat{g}_1(t)$ and $\widehat{g}_2(t)$ are estimates of $g_1(t)$ and $g_2(t)$, under the action of disturbance observers, the errors between them are also bounded. Thus, there exist positive numbers ζ_3 and ζ_4, satisfying $|\widetilde{g}_1(t)| \le \zeta_3$ and $|\widetilde{g}_2(t)| \le \zeta_4$.

Let $\mu_1 = k_2 - (1/\eta_9) > 0$ and $\mu_2 = k_1 - (1/\eta_8) > 0$. The selection of intermediate parameters is provided as follows:

$$\mu_3 = \frac{b\xi EI_b}{2s^4} - \eta_1 b - a\rho - 2a\rho x_e c\eta_5 > 0,$$

$$\mu_4 = \frac{b\xi GJ}{2s^2} - \eta_2 b x_a c - aI_p - \frac{2a\rho x_e c}{\eta_5} > 0,$$

$$\mu_5 = aEI_b - \frac{a\xi EI_b}{\eta_3} - \eta_6 a s^4 > 0,$$

$$\mu_6 = aGJ - \frac{a\xi GJ}{\eta_4} - \eta_7 a s_2 x_a c > 0,$$

$$\lambda_3 = \min\{\mu_3, \mu_4, \mu_5, \mu_6\} > 0,$$

$$\varepsilon = \left(\frac{b}{\eta_1} + \frac{bx_a c}{\eta_2} + \frac{a}{\eta_6} + \frac{ax_a c}{\eta_7}\right) s g_{h\max}^2 + \eta_9 \zeta_4^2 + \eta_8 \zeta_3^2 < +\infty. \tag{32}$$

Therefore, we can obtain

$$\dot{W}(t) \le -\lambda W(t) + \varepsilon, \tag{33}$$

where $\lambda = \lambda_3/\lambda_1$.

Theorem 2. *Through the dynamical system and the proposed control laws, the controlled system's states $q(z,t)$ and $\theta(z,t)$ are uniformly ultimately bounded.*

Proof. Invoking (33) and multiplying $e^{\lambda t}$ yields

$$\dot{W}(t)e^{\lambda t} \le -\lambda W(t)e^{\lambda t} + \varepsilon e^{\lambda t}. \tag{34}$$

Integrating (34), we have

$$W(t) \le \left[W(0) - \frac{\varepsilon}{\lambda}\right]e^{-\lambda t} + \frac{\varepsilon}{\lambda} \le W(0)e^{-\lambda t} + \frac{\varepsilon}{\lambda}. \tag{35}$$

Furthermore, invoking (24) and Lemma 2, we have

$$\begin{aligned} \frac{1}{s^3}[q(z,t)]^2 &\le \frac{1}{s^2}\int_0^s [q'(z,t)]^2 \mathrm{d}z \\ &\le \int_0^s [q''(z,t)]^2 \mathrm{d}z \le \kappa(t) \le \frac{1}{\lambda} W(t). \end{aligned} \tag{36}$$

Finally, this results in

$$\begin{aligned} |q(z,t)| &\le \sqrt{\frac{s^3}{\lambda_2}\left(W(0)e^{-\lambda t} + \frac{\varepsilon}{\lambda}\right)}, \forall (z,t) \in [0,s] \times [0,+\infty), \\ |\theta(z,t)| &\le \sqrt{\frac{s}{\lambda_2}\left(W(0)e^{-\lambda t} + \frac{\varepsilon}{\lambda}\right)}, \forall (z,t) \in [0,s] \times [0,+\infty). \end{aligned} \tag{37}$$

□

Theorem 3. *Provided that $\kappa_2 \ge \zeta_1$ holds, the disturbance error $\widetilde{g}_1(t)$ ensures convergence to zero before $t \ge t_{f1}$, where*

$$t_{f1} \le \frac{a_2}{2\kappa_1(a_2 - a_1)} \ln\left\{\frac{\kappa_1 Q_1^{a_2 - a_1/a_2}(0) + 2^{(a_1/a_2)-1}\kappa_3}{2^{a_1/a_2 - 1}\kappa_3}\right\}, \tag{38}$$

with $Q_1(0)$ denoting an initial value of $Q_1(t)$, and $Q_1(t) = \sigma_1^2(t)/2$

Theorem 4. *Provided that $\kappa_5 \ge \zeta_2$ holds, the disturbance error $\widetilde{g}_2(t)$ converges to zero before $t \ge t_{f2}$, where*

$$t_{f2} \le \frac{b_2}{2\kappa_4(b_2 - b_1)} \ln\left\{\frac{\kappa_4 Q_2^{b_2 - b_1/b_2}(0) + 2^{(b_1/b_2)-1}\kappa_6}{2^{b_1/b_2 - 1}\kappa_6}\right\}, \tag{39}$$

with $Q_2(0)$ denoting an initial value of $Q_2(t)$, and $Q_2(t) = \sigma_2^2(t)/2$.

Proof. Differentiating $Q_1(t)$ and invoking (16) and (17), we have

$$\begin{aligned} \dot{Q}_1(t) &= \sigma_1(t)\dot{\sigma}_1(t) \\ &= \sigma_1(t)\left[\xi EI_b \dot{q}'''(s,t) - \dot{\nu}_1(t)\right] \\ &= \sigma_1(t)\left[\xi EI_b \dot{q}'''(s,t) - \kappa_1\phi_1(t) - \kappa_2 \mathrm{sign}(\phi_1(t)) - \kappa_3 \sigma_1^{2a_1 - a_2/a_2}(t) - \tau_1(t) - EI_b q(s,t)\right] \\ &= -\kappa_1\sigma_1^2(t) - \kappa_2|\sigma_1(t)| - \kappa_3\sigma_1(t)^{2a_1 - a_2/a_2}(t) + \sigma_1(t) + g_1(t) \\ &\le -\kappa_1\sigma_1^2(t) - (\kappa_2 - \zeta_1)|\sigma_1(t)| - \kappa_3\phi_1(t)\sigma_1^{2a_1 - a_2/a_2}(t) \\ &\le -\kappa_1\sigma_1^2(t) - \kappa_3\sigma_1(t)\sigma_1^{2a_1 - a_2/a_2}(t). \end{aligned} \tag{40}$$

Therefore, $Q_1(t)$ will converge to an equilibrium point in a finite time t_{f1}. We define $p = a_1/a_2$, and then we multiply (40) by $Q_1^p(t)/(1-p)$ to derive the following:

$$dQ_1 \le \frac{\left\{-2\kappa_1(1-p)Q_1^{1-p}(t) - 2^p\kappa_3(1-p)\right\}Q_1^p(t)}{((1-p)\mathrm{d}t)}. \tag{41}$$

Letting $\iota(t) = Q_1^{1-p}(t)$, with the analysis made in (41), we derive

$$\dot{\iota}(t) \leq -2\kappa_1(1-p)\iota(t) - 2^p\kappa_3(1-p). \tag{42}$$

Multiplying (42) by $e^{2\kappa_1(1-p)t}$ results in

$$\begin{aligned}\dot{\iota}(t)e^{2\kappa_1(1-p)t} \leq\ & -2\kappa_1(1-p)e^{2\kappa_1(1-p)t}\iota(t) \\ & -2^p\kappa_3(1-p)e^{2\kappa_1(1-p)t}.\end{aligned} \tag{43}$$

Then, we obtain

$$\frac{d\left(\iota(t)e^{2\kappa_1(1-p)t}\right)}{dt} \leq -2^p\kappa_3(1-p)e^{2\kappa_1(1-p)t}. \tag{44}$$

We apply the integral of (44) as follows:

$$\iota(t) \leq -\frac{2^{(p-1)}\kappa_3}{\kappa_1} + \left\{\iota(0) + \frac{2^{(p-1)}\kappa_3}{\kappa_1}\right\}e^{-2\kappa_1(1-p)t}. \tag{45}$$

Equation (45) can be rewritten as

$$Q^{1-p}(t) \leq -\frac{2^{(p-1)}\kappa_3}{\kappa_1} + \left\{Q_1^{1-p}(0) + \frac{2^{(p-1)}\kappa_3}{\kappa_1}\right\}e^{-2\kappa_1(1-p)t}. \tag{46}$$

Invoking $Q_1(t)$ and (40) yields

$$Q_1(t) \geq 0, \dot{Q}_1(t) \leq 0. \tag{47}$$

According to (46) and (47), we have

$$\left\{Q_1^{1-p}(0) + \frac{2^{(p-1)}\kappa_3}{\kappa_1}\right\}e^{-2\kappa_1(1-p)t_{f1}} - \frac{2^{(p-1)}\kappa_3}{\kappa_1} \geq 0. \tag{48}$$

When $t = t_{f1}$ and $Q_1(t_{f1}) = 0$, then we have $Q_1(t) \equiv 0$. We can further obtain

$$e^{2\kappa_1(1-p)t_{f1}} \leq \frac{\kappa_1 Q_1^{1-p}(0) + 2^{(p-1)}\kappa_3}{2^{(p-1)}\kappa_3}. \tag{49}$$

Taking the logarithm for it as follows:

$$\begin{aligned}t_{f1} &\leq \frac{1}{2\kappa_1(1-p)}\ln\left\{\frac{\kappa_1 Q_1^{1-p}(0) + 2^{(p-1)}\kappa_3}{2^{(p-1)}\kappa_3}\right\} \\ &= \frac{a_2}{2\kappa_1(a_2-a_1)}\ln\left\{\frac{\kappa_1 Q_1^{a_2-a_1/a_2}(0) + 2^{a_1/a_2} - 1\kappa_3}{2^{a_1/a_2-1}\kappa_3}\right\}.\end{aligned} \tag{50}$$

In a word, considering $\kappa_2 \geq \zeta_1$, when $t \geq t_{f1}$, we derive

$$Q_1(t) \equiv 0. \tag{51}$$

Invoking (51) and $Q_1(t)$, we obtain the following when $t \geq t_{f1}$,

$$\sigma_1(t) \equiv 0. \tag{52}$$

Moreover, when $t \geq t_{f1}$, we arrive at

$$\dot{\sigma}_1(t) \equiv 0. \tag{53}$$

The disturbance estimation error is expressed as follows:

$$\tilde{g}_1(t) = g_1(t) - \hat{g}_1(t). \tag{54}$$

The combination of (10), (20), and (54) gives

$$\begin{aligned}\dot{\tilde{g}}_1(t) &= -\tau_1(t) - \xi EI_b\dot{q}'''(s,t) - EI_b q'''(s,t) - \dot{\hat{g}}_1(t) \\ &= -\xi EI_b\dot{q}'''(s,t) + \left\{-\tau_1(t) - \left(EI_b q'''(s,t) + \kappa_1\sigma_1(t)\right.\right. \\ &\quad \left.\left. + \kappa_2\text{sign}\left(\sigma_1(t) + \kappa_3\sigma_1^{2a_1-a_2/a_2}\right)\right)\right\} \\ &= \dot{\sigma}_1(t).\end{aligned} \tag{55}$$

Invoking (53) and (55), we can conclude that if $\kappa_2 \geq \zeta_1$ holds, $\tilde{g}_1(t)$ converges to zero for $\forall t \geq t_{f1}$. Similarly, we can prove that if $\kappa_5 \geq \zeta_2$ holds, $\tilde{g}_2(t)$ converges to zero for $\forall t \geq t_{f2}$. □

4. Simulation

In this section, the finite difference method is used to approximate the dynamics of the system with system parameters as $s = 2.0\,m$, $x_e c = 0.35m$, $EI_b = 0.2Nm^2$, $GJ = 0.5Nm^2$, $\rho = 10kg/m$, $x_a c = 0.05N$, $I_p = 1.5$kgm, and $\xi = 0.6$. The initial condition of the system is set as $q(z,0) = z/s$, and $\theta(z,0) = (\pi z/2s)$. Besides, we have $\dot{q}(z,0) = 0$ and $\dot{\theta}(z,0) = 0$. The inevitable external disturbances are defined as follows:

$$\begin{aligned}g_h(z,t) &= (1 + +3\,\cos(3\pi t) + \sin(\pi t))z/30 \\ g_1(t) &= 0.02 + 0.06\,\sin(0.05t) \\ g_2(t) &= 0.04 + 0.02\,\sin(0.1t).\end{aligned} \tag{56}$$

Figures 3 and 4 show the displacement of the coupled wing without control, that is, $\tau_1(t) = 0$ and $\tau_2(t) = 0$. Figures 5 and 6 depict the three-dimensional representation of flexible wings with boundary control. The control parameters are chosen as $k_1 = 2$, $k_2 = 1$, $\kappa_1 = 0.8$, $\kappa_2 = 1$, $\kappa_3 = 4$, $\kappa_4 = 0.8$, $\kappa_5 = 1$, $\kappa_6 = 4$, $a_1 = b_1 = 7$, and $a_2 = b_2 = 13$. Figures 7 and 8 represent the response generated by the control inputs $\tau_1(t)$ and $\tau_2(t)$. As shown in Figures 9 and 10, we can conclude that the control design can ensure that the flexible wing system has good performance by comparing with the freely vibrating situation. At last, we provide two pictures Figures 11 and 12 about the disturbance estimation errors. It can be concluded from the figures that the disturbance estimation errors can converge to zero in a finite time.

The simulation results Figures 3–12 show that the designed controller can effectively suppress the vibration of flexible wing, and the bending and torsion deformation of a flexible wing $q(z,t)$ and $\theta(z,t)$ under the presented control are guaranteed to be stable. The last two figures show the finite-time convergence of the disturbance estimation errors $\tilde{g}_1(t)$ and $\tilde{g}_2(t)$. In order to further highlight the advantages of the proposed control strategy, a boundary control strategy based on the nonlinear disturbance observers (DOBC) is expressed as follows:

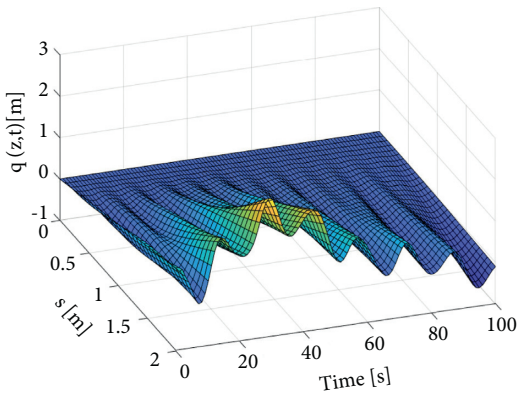

Figure 3: Bending displacement of the wing without control.

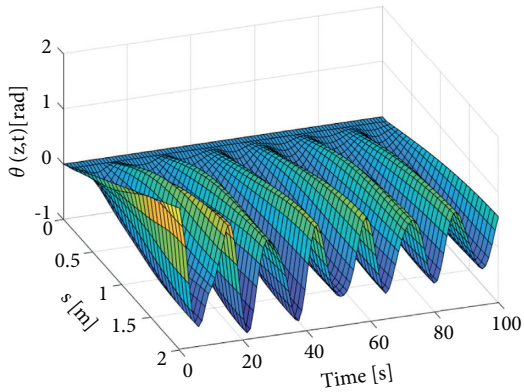

Figure 4: Twist displacement of the wing under without control.

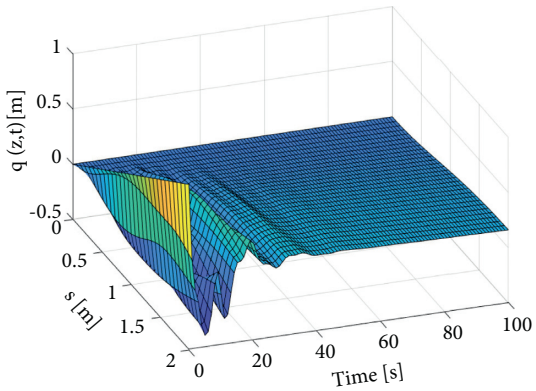

Figure 5: Bending displacement of the wing with the proposed control.

$$
\begin{aligned}
\tau_1(t) &= -k_1[aq(s,t) + b\dot{q}(s,t)] - \hat{g}_1(t),\\
\tau_2(t) &= -k_2[a\theta(s,t) + b\dot{\theta}(s,t)] - \hat{g}_2(t),\\
\hat{g}_1(t) &= -\xi EIq'''(s,t) + \sigma_1(t),\\
\dot{\sigma}_1(t) &= -\tau_1(t) - EI_b q'''(s,t) - \hat{g}_1(t),\\
\hat{g}_2(t) &= \xi GJ\theta'(s,t) + \sigma_2(t),\\
\dot{\sigma}_2(t) &= -\tau_2(t) + GJ\theta'(s,t) - \hat{g}_2(t),
\end{aligned}
\tag{57}
$$

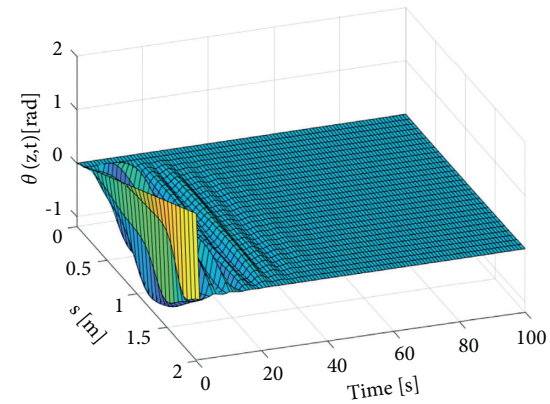

Figure 6: Twist displacement of the wing with the proposed control.

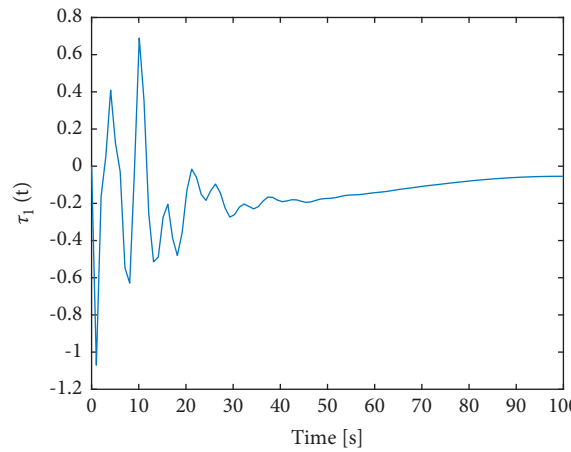

Figure 7: Designed control command $\tau_1(t)$ with the proposed control.

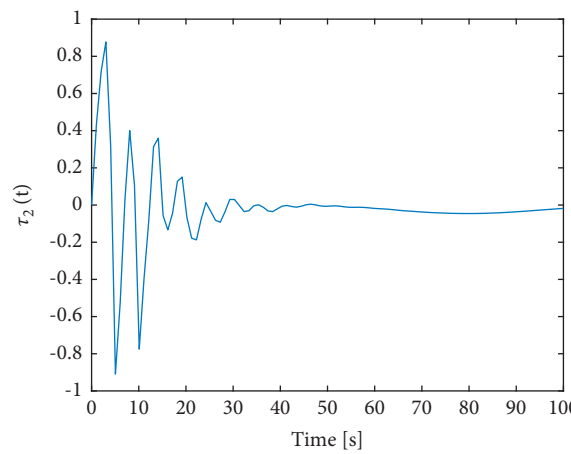

Figure 8: Designed control command $\tau_2(t)$ with the proposed control.

where parameter selections are consistent with the above design. Figures 13–20 show the control effect of the system using the DOBC strategy. It can be seen that the control

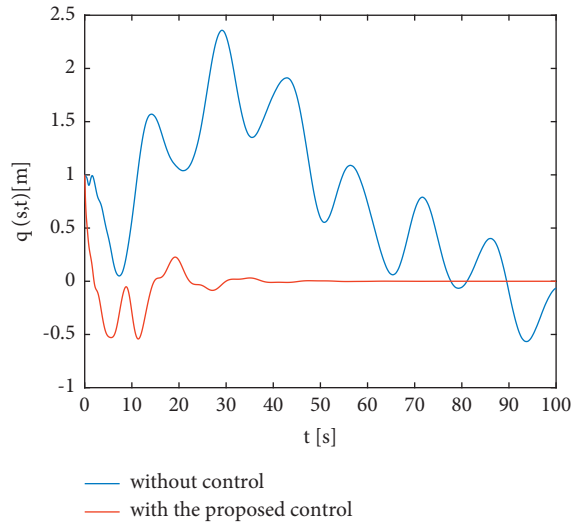

Figure 9: Boundary bending displacement of the wing with the proposed control.

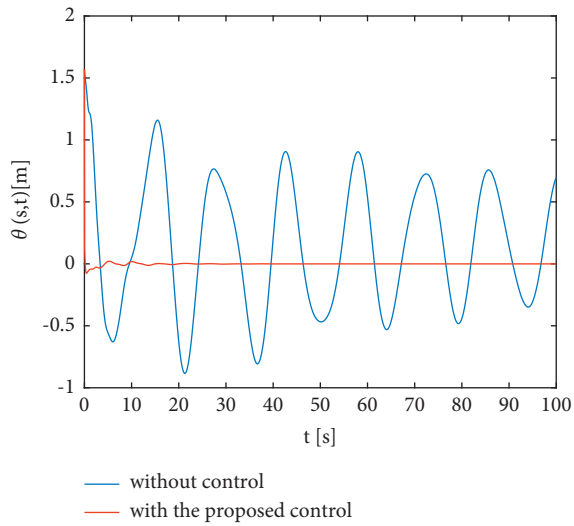

Figure 10: Boundary twist displacement of the wing with the proposed control.

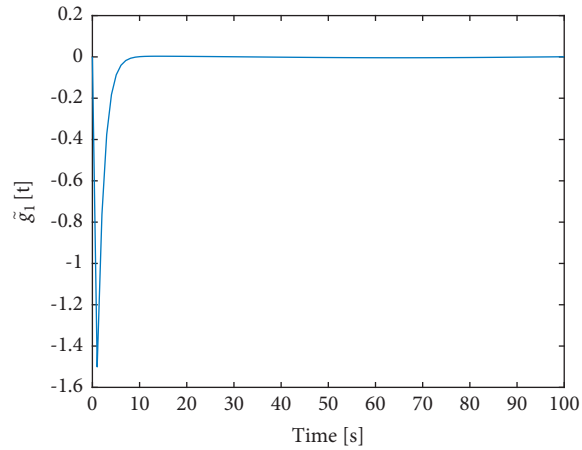

Figure 11: Disturbance estimation error $\tilde{g}_1(t)$ with the proposed control.

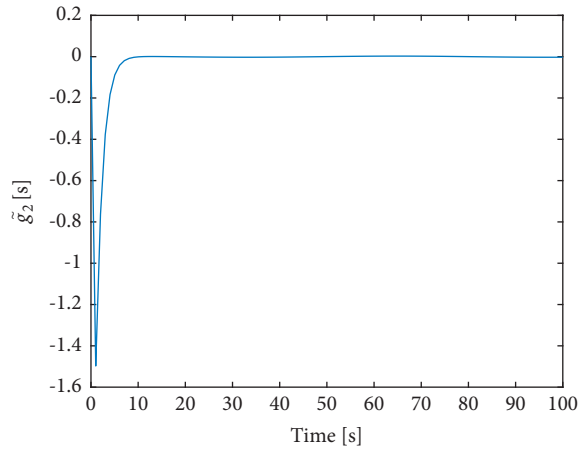

Figure 12: Disturbance estimation error $\tilde{g}_2(t)$ with the proposed control.

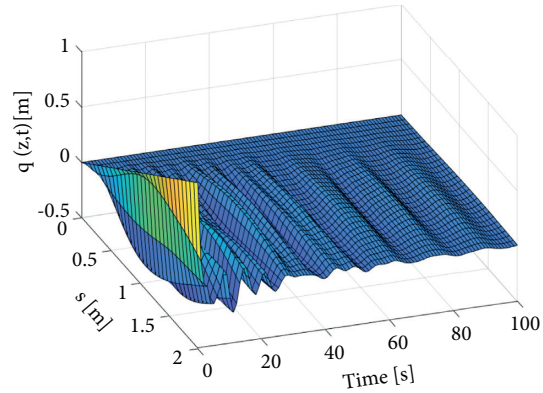

Figure 13: Bending displacement of the wing with DOBC.

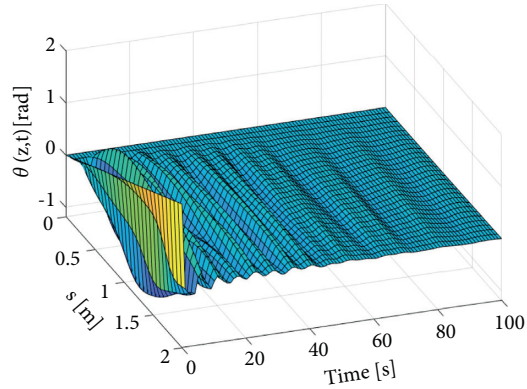

Figure 14: Twist displacement of the wing with DOBC.

effect is worse than that of the control strategy proposed in this paper. As can be seen from the figures, the inputs $\tau_1(t)$ and $\tau_2(t)$ and displacements $q(z,t)$, $\theta(z,t)$, $q(s,t)$, and $\theta(s,t)$ cannot converge to zero quickly. Although the disturbance observers can track the change of external disturbances to a certain extent, they will still produce a certain disturbance errors. To sum up, we can get that the control

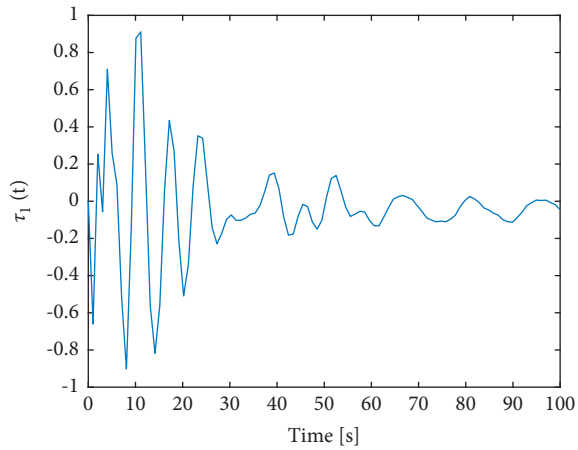

Figure 15: Designed control command $\tau_1(t)$ with DOBC.

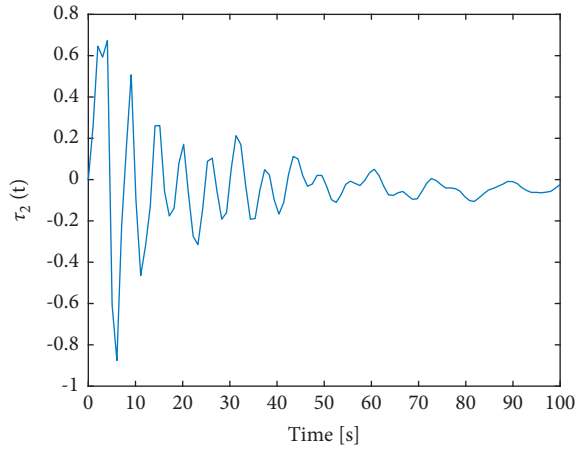

Figure 16: Designed control command $\tau_2(t)$ with DOBC.

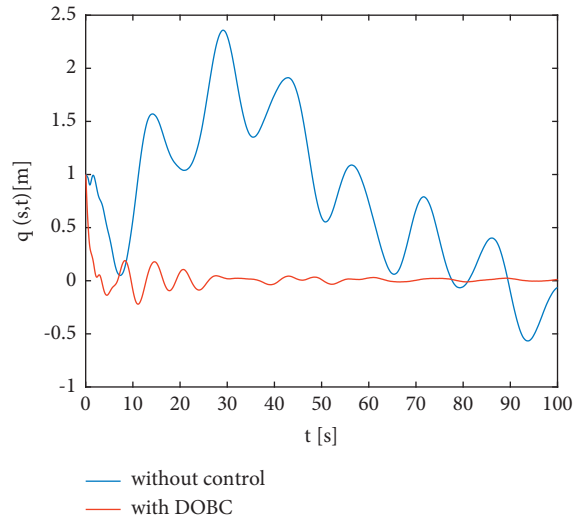

Figure 17: Boundary bending displacement of the wing with DOBC.

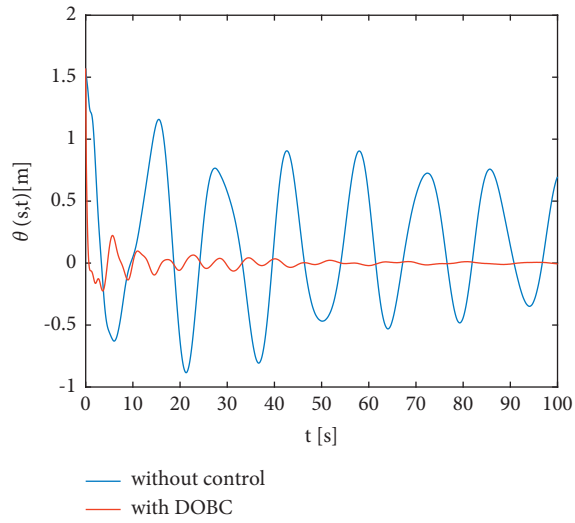

Figure 18: Boundary twist displacement of the wing with DOBC.

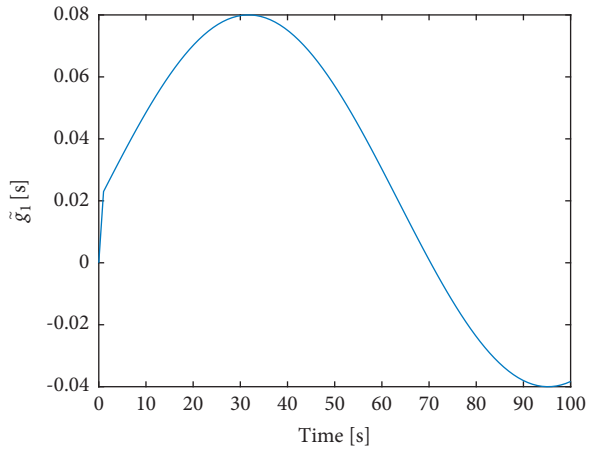

Figure 19: Disturbance estimation error $\tilde{g}_1(t)$ with DOBC.

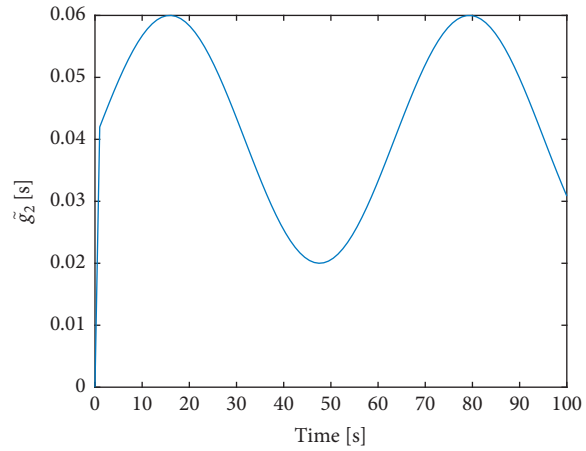

Figure 20: Disturbance estimation error $\tilde{g}_2(t)$ with DOBC.

effect of the derived finite-time convergence antidisturbance control strategy is better than that of the DOBC strategy.

5. Conclusion

In this paper, based on Lyapunov's direct method and the new coupled wing model, we addressed the control problem for the flexible wing subject to external disturbances with a new finite-time convergence antidisturbance control strategy. Under the action of the controllers, the external disturbance errors converged to zero in a finite time. Hence, we concluded that the proposed control scheme could stabilize the flexible wing system with a better performance. Finally, we analyzed the stability of the closed-loop system and the effectiveness of the boundary controller through strict theoretical proof and simulation results. Future research directions may include the adaptive control [50–53], intelligent techniques [54–57], and the uncertainty and disturbance estimator-based control [58–60].

Data Availability

The data used to support the results of this study are available from the first author (1707700028@e.gzhu.edu.cn).

Conflicts of Interest

The authors declare that they have no conflicts of interest.

Acknowledgments

This work was supported in part by the Innovative School Project of Education Department of Guangdong (202011078022).

References

[1] K. Y. Ma, P. Chirarattananon, S. B. Fuller, and R. J. Wood, "Controlled flight of a biologically inspired, insect-scale robot," *Science*, vol. 340, no. 6132, pp. 603–607, 2013.

[2] M. Hamamoto, Y. Ohta, K. Hara, and T. Hisada, "A fundamental study of wing actuation for a 6-in-wingspan flapping microaerial vehicle," *IEEE Transactions on Robotics*, vol. 26, no. 2, pp. 244–255, 2010.

[3] G. K. Lau, Y. W. Chin, J. T. W. Goh, and R. J. Wood, "Dipteran-insect-inspired thoracic mechanism with nonlinear stiffness to save inertial power of flapping-wing flight," *IEEE Transactions on Robotics*, vol. 30, no. 5, pp. 1187–1197, 2014.

[4] A. A. Paranjape, S. J. Chung, and J. Kim, "Novel dihedral-based control of flapping-wing aircraft with application to perching," *IEEE Transactions on Robotics*, vol. 29, no. 5, pp. 1071–1084, 2013.

[5] W. He, Z. Yan, C. Sun, and Y. Chen, "Adaptive neural network control of a flapping wing micro aerial vehicle with disturbance observer," *IEEE Transactions on Cybernetics*, vol. 47, no. 10, pp. 3452–3465, 2017.

[6] W. He, X. Mu, L. Zhang, and Y. Zou, "Modeling and trajectory tracking control for flapping-wing micro aerial vehicles," *IEEE/CAA Journal of Automatica Sinica*, vol. 8, no. 1, pp. 148–156, 2020.

[7] M. H. Dickinson, F. O. Lehmann, and S. P. Sane, "Wing rotation and the aerodynamic basis of insect flight," *Science*, vol. 284, no. 5422, pp. 1954–1960, 1999.

[8] X. Xing and J. Liu, "Vibration and position control of overhead crane with three-dimensional variable length cable subject to input amplitude and rate constraints," *IEEE Transactions on Systems, Man, and Cybernetics: Systems*, vol. 51, 2019.

[9] S. Zhang, Y. Wu, X. He, and Z. Liu, "Cooperative fault-tolerant control for a mobile dual flexible manipulator with output constraints," *IEEE Transactions on Automation Science and Engineering*, 2021.

[10] S. Gao and J. Liu, "Adaptive neural network vibration control of a flexible aircraft wing system with input signal quantization," *Aerospace Science and Technology*, vol. 96, Article ID 105593, 2020.

[11] H. N. Wu and J. W. Wang, "Static output feedback control via PDE boundary and ODE measurements in linear cascaded ODE-beam systems," *Automatica*, vol. 50, no. 11, pp. 2787–2798, 2014.

[12] Y. Ren, M. Chen, and J. Liu, "Unilateral boundary control for a suspension cable system of a helicopter with horizontal motion," *IET Control Theory & Applications*, vol. 13, no. 4, pp. 467–476, 2018.

[13] Z. Zhao, Z. Liu, W. He, K. S. Hong, and H. X. Li, "Boundary adaptive fault-tolerant control for a flexible Timoshenko arm with backlash-like hysteresis," *Automatica*, vol. 130, Article ID 109690, 2021.

[14] U. H. Shah and K. S. Hong, "Active vibration control of a flexible rod moving in water: application to nuclear refueling machines," *Automatica*, vol. 93, pp. 231–243, 2018.

[15] C. Sun, W. He, and J. Hong, "Neural network control of a flexible robotic manipulator using the lumped spring-mass model," *IEEE Transactions on Systems, Man, and Cybernetics: Systems*, vol. 47, no. 8, pp. 1863–1874, 2016.

[16] D. Zhao, B. Jiang, H. Yang, and G. Tao, "A sliding mode fault compensation scheme for a coupled rigid-flexible system in PDE-ODE form," *Journal of the Franklin Institute*, vol. 357, no. 14, pp. 9174–9194, 2020.

[17] Z. Zhao, X. He, Z. Ren, and G. Wen, "Boundary adaptive robust control of a flexible riser system with input nonlinearities," *IEEE Transactions on Systems, Man, and Cybernetics: Systems*, vol. 49, no. 10, pp. 1971–1980, 2018.

[18] M. Chen, Y. Ren, and J. Liu, "Antidisturbance control for a suspension cable system of helicopter subject to input nonlinearities," *IEEE Transactions on Systems, Man, and Cybernetics: Systems*, vol. 48, no. 12, pp. 2292–2304, 2017.

[19] L. Su, J. M. Wang, and M. Krstic, "Boundary feedback stabilization of a class of coupled hyperbolic equations with nonlocal terms," *IEEE Transactions on Automatic Control*, vol. 63, no. 8, pp. 2633–2640, 2017.

[20] B. D. A. Novel and J. M. Coron, "Exponential stabilization of an overhead crane with flexible cable via a back-stepping approach," *Automatica*, vol. 36, no. 4, pp. 587–593, 2000.

[21] W. He, T. Meng, X. He, and S. S. Ge, "Unified iterative learning control for flexible structures with input constraints," *Automatica*, vol. 96, 2018.

[22] G. Zhu, S. S. Ge, and T. H. Lee, "Simulation studies of tip tracking control of a single-link flexible robot based on a lumped model," *Robotica*, vol. 17, no. 1, pp. 71–78, 1999.

[23] Z. Zhao and Z. Liu, "Finite-time convergence disturbance rejection control for a flexible Timoshenko manipulator," *IEEE/CAA Journal of Automatica Sinica*, vol. 8, no. 1, pp. 157–168, 2020.

[24] Y. Ma, X. He, M. Chen, and W. He, "Predictor-based control for a flexible satellite subject to output time delay," *IEEE Transactions on Control Systems Technology*, 2021.

[25] X. He, Y. Song, Z. Han, S. Zhang, P. Jing, and S. Qi, "Adaptive inverse backlash boundary vibration control design for an Euler-Bernoulli beam system," *Journal of the Franklin Institute*, vol. 357, no. 6, pp. 3434–3450, 2020.

[26] Z. Zhao and C. K. Ahn, "Boundary output constrained control for a flexible beam system with prescribed performance," *IEEE Transactions on Systems, Man, and Cybernetics: Systems*, vol. 51, 2019.

[27] Y. Liu, X. Chen, Y. Mei, and Y. Wu, "Observer-based boundary control for an asymmetric output-constrained flexible robotic manipulator," *Science China Information Sciences*, vol. 65, no. 3, pp. 1–3, 2020.

[28] G. Ma, Z. Tan, Y. Liu, Z. Zhao, and T. Zou, "Adaptive robust barrier-based control of a 3D flexible riser system subject to boundary displacement constraints," *International Journal of Robust and Nonlinear Control*, 2021.

[29] Z. Liu, J. Shi, X. Zhao, Z. Zhao, and H. X. Li, "Adaptive fuzzy event-triggered control of aerial refueling hose system with actuator failures," *IEEE Transactions on Fuzzy Systems*, 2021.

[30] X. He, Z. Zhao, and Y. Song, "Active control for flexible mechanical systems with mixed deadzone-saturation input nonlinearities and output constraint," *Journal of the Franklin Institute*, vol. 356, no. 9, pp. 4749–4772, 2019.

[31] Z. Liu, X. He, Z. Zhao, C. K. Ahn, and H. X. Li, "Vibration control for spatial aerial refueling hoses with bounded actuators," *IEEE Transactions on Industrial Electronics*, vol. 68, 2020.

[32] S. Zhang, W. He, and D. Huang, "Active vibration control for a flexible string system with input backlash," *IET Control Theory & Applications*, vol. 10, no. 7, pp. 800–805, 2016.

[33] Z. Zhao, C. K. Ahn, and H. X. Li, "Boundary antidisturbance control of a spatially nonlinear flexible string system," *IEEE Transactions on Industrial Electronics*, vol. 67, no. 6, pp. 4846–4856, 2019.

[34] Z. Zhao, C. K. Ahn, and H. X. Li, "Dead zone compensation and adaptive vibration control of uncertain spatial flexible riser systems," *IEEE*, vol. 25, no. 3, pp. 1398–1408, 2020.

[35] Z. Zhao, Y. Ren, C. Mu, T. Zou, and K. S. Hong, "Adaptive neural-network-based fault-tolerant control for a flexible string with composite disturbance observer and input constraints," *IEEE Transactions on Cybernetics*, 2021.

[36] W. He, T. Meng, X. He, and C. Sun, "Iterative learning control for a flapping wing micro aerial vehicle under distributed disturbances," *IEEE Transactions on Cybernetics*, vol. 49, no. 4, pp. 1524–1535, 2018.

[37] A. A. Paranjape, J. Guan, S. J. Chung, and M. Krstic, "PDE boundary control for flexible articulated wings on a robotic aircraft," *IEEE Transactions on Robotics*, vol. 29, no. 3, pp. 625–640, 2013.

[38] W. He and S. Zhang, "Control design for nonlinear flexible wings of a robotic aircraft," *IEEE Transactions on Control Systems Technology*, vol. 25, no. 1, pp. 351–357, 2016.

[39] W. He, T. Wang, X. He, L. J. Yang, and O. Kaynak, "Dynamical modeling and boundary vibration control of a rigid-flexible wing system," *IEEE*, vol. 25, no. 6, pp. 2711–2721, 2020.

[40] B. Xu, D. Wang, Y. Zhang, and Z. Shi, "DOB-based neural control of flexible hypersonic flight vehicle considering wind effects," *IEEE Transactions on Industrial Electronics*, vol. 64, no. 11, pp. 8676–8685, 2017.

[41] M. Chen and J. Yu, "Disturbance observer-based adaptive sliding mode control for near-space vehicles," *Nonlinear Dynamics*, vol. 82, no. 4, pp. 1671–1682, 2015.

[42] S. Shao, M. Chen, J. Hou, and Q. Zhao, "Event-triggered-based discrete-time neural control for a quadrotor UAV using disturbance observer," *IEEE*, vol. 26, no. 2, pp. 689–699, 2021.

[43] Z. Zhao, X. He, and C. K. Ahn, "Boundary disturbance observer-based control of a vibrating single-link flexible manipulator," *IEEE Transactions on Systems, Man, and Cybernetics: Systems*, vol. 51, 2019.

[44] Y. Zhang, J. Liu, and W. He, "Disturbance observer design and vibration control for a flexible aircraft wing," *Transactions of the Institute of Measurement and Control*, vol. 40, no. 13, pp. 3760–3773, 2018.

[45] H. Yang, J. Liu, and W. He, "Distributed disturbance-observer-based vibration control for a flexible-link manipulator with output constraints," *Science China Technological Sciences*, vol. 61, no. 10, pp. 1528–1536, 2018.

[46] M. V. Basin, F. G. Avellaneda, and Y. B. Shtessel, "Stock management problem: adaptive fixed-time convergent continuous controller design," *IEEE Transactions on Systems, Man, and Cybernetics: Systems*, vol. 50, no. 12, pp. 4974–4983, 2019.

[47] S. S. Ge, W. He, B. V. E. How, and Y. S. Choo, "Boundary control of a coupled nonlinear flexible marine riser," *IEEE Transactions on Control Systems Technology*, vol. 18, no. 5, pp. 1080–1091, 2009.

[48] W. He, X. Mu, Y. Chen, X. He, and Y. Yu, "Modeling and vibration control of the flapping-wing robotic aircraft with output constraint," *Journal of Sound and Vibration*, vol. 423, pp. 472–483, 2018.

[49] C. D. Rahn, *Mechatronic Control of Distributed Noise and Vibration*, Springer-Verlag, New York, NY, USA, 2001.

[50] C. Yang, Y. Jiang, J. Na, Z. Li, L. Cheng, and C. Y. Su, "Finite-time convergence adaptive fuzzy control for dual-arm robot with unknown kinematics and dynamics," *IEEE Transactions on Fuzzy Systems*, vol. 27, no. 3, pp. 574–588, 2018.

[51] Z. Zhao, Y. Liu, T. Zou, and K. S. Hong, "Robust adaptive control of a riser-vessel system in three-dimensional space," *IEEE Transactions on Systems, Man, and Cybernetics: Systems*, 2021.

[52] C. Yang, C. Chen, W. He, R. Cui, and Z. Li, "Robot learning system based on adaptive neural control and dynamic movement primitives," *IEEE Transactions on Neural Networks and Learning Systems*, vol. 30, no. 3, pp. 777–787, 2018.

[53] N. Wang, C. Chen, and C. Yang, "A robot learning framework based on adaptive admittance control and generalizable motion modeling with neural network controller," *Neurocomputing*, vol. 390, pp. 260–267, 2020.

[54] C. Yang, D. Huang, W. He, and L. Cheng, "Neural control of robot manipulators with trajectory tracking constraints and input saturation," *IEEE Transactions on Neural Networks and Learning Systems*, vol. 32, 2020.

[55] C. Yang, G. Peng, L. Cheng, J. Na, and Z. Li, "Force sensorless admittance control for teleoperation of uncertain robot manipulator using neural networks," *IEEE Transactions on Systems, Man, and Cybernetics: Systems*, vol. 51, 2019.

[56] Y. Liu, X. Chen, Y. Wu, H. Cai, and H. Yokoi, "Adaptive neural network control of a flexible spacecraft subject to input nonlinearity and asymmetric output constraint," *IEEE Transactions on Neural Networks and Learning Systems*, 2021.

[57] C. Liu, G. Wen, Z. Zhao, and R. Sedaghati, "Neural-network-based sliding-mode control of an uncertain robot using

dynamic model approximated switching gain," *IEEE Transactions on Cybernetics*, vol. 51, no. 5, pp. 2339–2346, 2020.

[58] J. Dai and B. Ren, "UDE-based robust boundary control for an unstable parabolic PDE with unknown input disturbance," *Automatica*, vol. 93, pp. 363–368, 2018.

[59] Y Dong and B. Ren, "UDE-based variable impedance control of uncertain robot systems," *IEEE Transactions on Systems, Man, and Cybernetics: Systems*, vol. 49, no. 12, pp. 2487–2498, 2017.

[60] Q. C. Zhong, Y. Wang, and B. Ren, "UDE-based robust droop control of inverters in parallel operation," *IEEE Transactions on Industrial Electronics*, vol. 64, no. 9, pp. 7552–7562, 2017.